J Paleolimnol (2013) 49:619–631
DOI 10.1007/s10933-013-9679-9

ORIGINAL PAPER

Increased precipitation during the Little Ice Age in northern Taiwan inferred from diatoms and geochemistry in a sediment core from a subalpine lake

Liang-Chi Wang · Hermann Behling · Teh-Quei Lee · Hong-Chun Li · Chih-An Huh · Liang-Jian Shiau · Su-Hwa Chen · Jiunn-Tzong Wu

Received: 9 January 2012 / Accepted: 8 January 2013 / Published online: 22 January 2013

Abstract We studied diatoms in a 55.5-cm-long sediment core from a subalpine lake in northern Taiwan, Tsuifong Lake (TFL), to investigate environmental changes from AD 490 to present. Diatom assemblages of the last century were dominated by acidophilous species, whereas alkaliphilous taxa dominated the record between AD 1480 and 1910. Over the studied time frame, four decadal periods with high precipitation were inferred from evidence of elevated soil input from the watershed, supported by the stable isotope signatures ($\delta^{15}N$, $\delta^{13}C$) of organic matter and magnetic susceptibility of the sediments. We compared the inferred changes in pH of TFL to values obtained from three other Taiwanese subalpine lakes. The present study revealed that elevated precipitation was associated with increased solar irradiance over the last five centuries, with a stable dry period between AD 490 and 1450. Acidification of TFL in the last ~100 years was a consequence of deforestation and acid rain.

Keywords Climate change · Diatom analysis · Acid precipitation · Little Ice Age · pH

Introduction

The Little Ice Age (LIA) was a multi-century climate anomaly that occurred between the fifteenth and nineteenth centuries and is observed as having been cold and dry in most paleoclimate reconstructions from the Northern Hemisphere (Grove 1988; Bradley and Jonest 1993). During that period, there was global glacial expansion and enhanced polar atmospheric circulation. The conventional view of a dry and cold climate during the LIA, however, is based largely on data from Western Europe and elsewhere in the North

L.-C. Wang · S.-H. Chen (✉)
Department of Life Science, National Taiwan University, Taipei 106, Taiwan
e-mail: suchen@ntu.edu.tw

L.-C. Wang · H. Behling
Department of Palynology and Climate Dynamics, Albrecht-von-Haller Institute for Plant Sciences, University of Göttingen, 37073 Göttingen, Germany

T.-Q. Lee · C.-A. Huh · L.-J. Shiau
Institute of Earth Sciences, Academia Sinica, Taipei 115, Taiwan

H.-C. Li
Department of Geosciences, National Taiwan University, Taipei 106, Taiwan

S.-H. Chen · J.-T. Wu
Institute of Ecology and Evolutionary Biology, National Taiwan University, Taipei 106, Taiwan

J.-T. Wu (✉)
Biodiversity Research Center, Academia Sinica, Taipei 115, Taiwan
e-mail: jtwu@gate.sinica.edu.tw

Atlantic region. This view has been challenged by findings of increased rainfall during the LIA in southern Norway (Nesje and Dahl 2003; Rasmussen et al. 2010), northern Patagonia, South America (Villalba 1994), southwest China (Chen et al. 2005), southern tropical China (Chu et al. 2002) and northern Taiwan (Chen et al. 2009; Wang et al. 2011). Such spatial variations in precipitation reflect the regional characteristics of climate, such as the East Asia monsoon. To improve understanding of the East Asia monsoon and global hydrology during the LIA, data from numerous sites are required.

Diatoms are sensitive indicators of changes in aquatic environments and have been used widely for inferring paleoenvironmental characteristics such as past temperature, pH, salinity, and nutrient concentrations (Stoermer and Smol 1999; Smol et al. 2001; Wu et al. 2001). Even extreme events such as floods and earthquakes can be identified using diatoms (Nelson et al. 1996; Kashima 2003; Atwater et al. 2004; Borromei et al. 2010; Schütt et al. 2010; Wiklund et al. 2010; Saegusa et al. 2011). Some environmental variables can be estimated quantitatively using diatom-based transfer functions (Shinneman et al. 2009, 2010).

Taiwan is located in a subtropical region, close to the boundary between the Pacific Ocean and Eurasia, and is strongly affected by monsoonal climate and summer typhoons. There are few inferred rainfall records for the Taiwan area that cover the last millennium. A few recent studies of lake sediments, however, provide some basic information on paleoclimate for this area (Wu et al. 1997; Lin et al. 2003, 2004, 2007; Chen et al. 2009). For this investigation, we conducted a paleolimnological study of Tsuifong Lake (TFL), involving analysis of diatoms, geochemistry and magnetic susceptibility (MS). The goal of this study was to obtain a high-resolution record of paleoclimate change in the region during the late Holocene. We focused on reconstructing paleoprecipitation in northeastern Taiwan during the last millennium.

Study site

Tsuifong Lake (24°30′N, 121°36′E) is the largest subalpine lake in northern Taiwan (Fig. 1). The water body extends NNW to SSE, and the southeast basin is somewhat larger and deeper than the northwest basin. The lake lies at an elevation of 1,840 m above sea level (a.s.l.) and is surrounded by yellow cypress forest composed of *Chamaecyparis formosensis* and *C. obtusa* var. *formosana*. The bedrock surrounding the lake is gray-black slate, with some thick layers of metamorphic sandstone and conglomerate (Integrated Geological Data Inquiry System, Central Geological Survey, MOEA, Taiwan).

The weather station nearest TFL, Taipingsan Weather Station (24°30′N, 121°31′E, 1,810 m a.s.l.), reports a mean annual temperature of 12.4 °C from data collected between 1996 and 2010. Mean January temperature is 6.1 °C and mean July temperature is 17.8 °C. Annual precipitation is 362 mm, with a range of 117–788 mm, and precipitation occurs primarily during the subtropical monsoon season, between July and October (Fig. 2).

The smaller NW basin of TFL is a seepage basin (Fig. 1). Its principal sources of water are direct precipitation and runoff, supplemented by groundwater from the small drainage area (Mao 2006). The maximum depth of TFL varies with the seasons, being ~3 m in the dry season (January to April) and ~7 m in the wet season (July to October). The depth may increase to 15 m as a consequence of flooding during typhoon events, when summer storms bring heavy rainfall within a short time period.

Lake surface waters are acidic (pH 5.6–6.7) in the dry season and slightly alkaline (pH 7.0–7.5) in the wet season. Bottom waters are acidic year-round (pH 5.8 at depth 4.7 m) (Mao 2006). Today, TFL is oligotrophic to mesotrophic. Lin (1996) documented deforestation for timber harvest between AD 1926 and 1982. There is no record of human disturbance in the watershed prior to that period.

Materials and methods

A 55.5-cm-long sediment core, TF-2, was taken from a boat in the southeastern part of TFL by pushing a 6-cm-diameter plastic pipe into the sediments (Fig. 1). The core was kept upright and stored in a dark, cold room (4 °C) before it was subsampled at 0.5-cm intervals in the laboratory. The lithology of the core is composed of fine-grained clay, without apparent laminations.

Samples in the upper 15 cm were evaluated for total ^{210}Pb activity at 0.5-cm intervals by measurement of

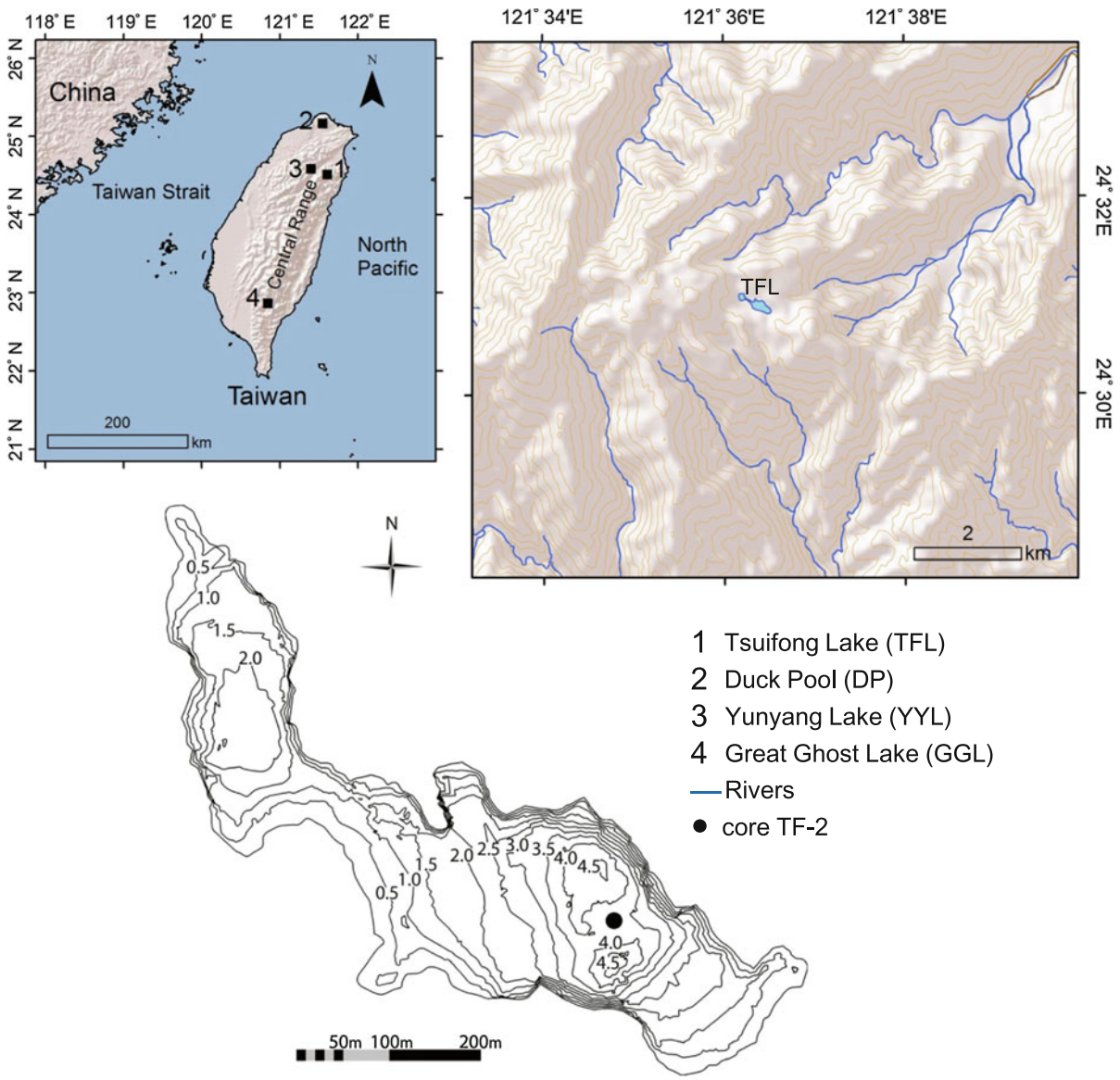

Fig. 1 Location of TFL (*1*) and its topography (*right*), showing the TF-2 core sampling site (*solid circle*). Locations of subalpine lakes Duck Pond (*2*), Yuanyang Lake (*3*), and Great Ghost Lake (*4*), for which paleolimnological data are also available

its granddaughter ^{210}Po, using α-spectrometry. Samples were counted for periods of 2–3 days, depending on the activity of ^{210}Po in the samples. ^{210}Pb dates were calculated using the constant rate of supply model (Binford 1990). Four plant fragments were dated by AMS ^{14}C at the laboratory of the Institute of Geological and Nuclear Sciences, New Zealand. Dates were calibrated using the program Calib 5.1 and the calibration curve IntCal04 (Reimer et al. 2004; Stuiver et al. 2005). Age/depth relations for the core were constructed by linear interpolation between dated depths below the basal ^{210}Pb date (Fig. 3).

Samples were prepared for diatom analysis according to methods described by Kashima (2003). Samples were treated with H_2O_2 to remove organic matter. Diatoms were mounted using Wako mounting media. At least 300 diatom valves were identified and counted in each sample using optical microscopy at 1,000× magnification. The identification of diatom species was based on references including Wang et al. (2010),

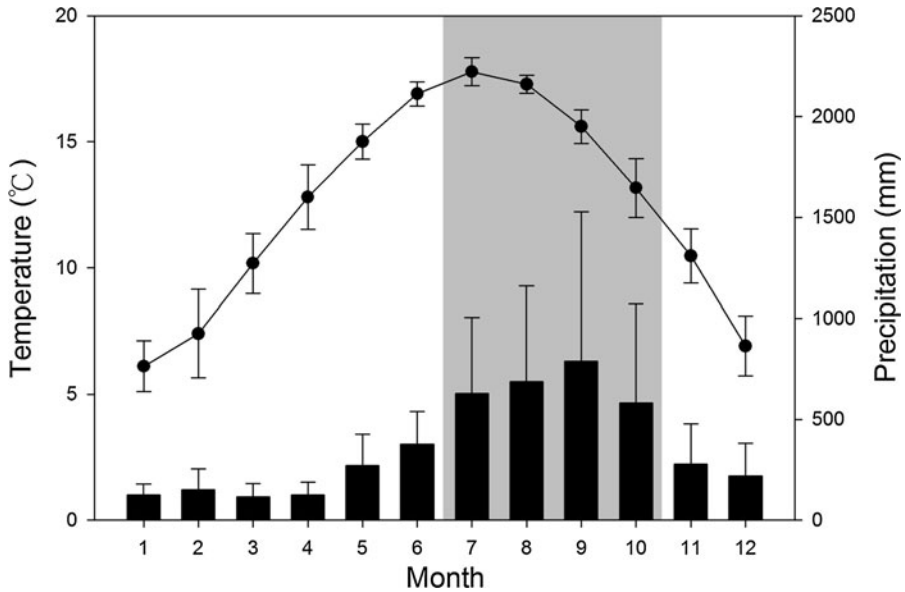

Fig. 2 Mean monthly temperature (*solid circles*) and precipitation (*bars*) data (1996–2010) from the Taipinshan weather station. The *shaded column* indicates the wet season

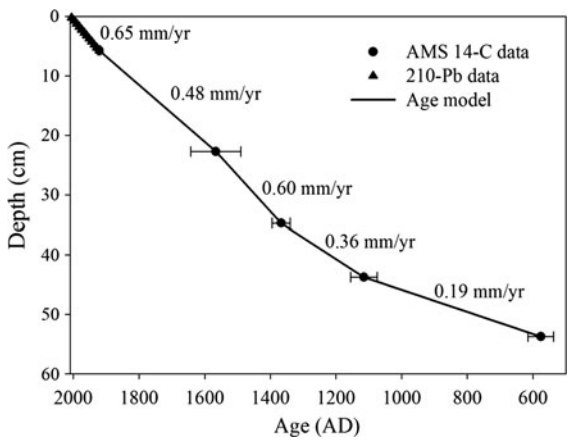

Fig. 3 Age-depth profile of the studied sediment core from TFL with dates and estimated sedimentation rates

Wu and Wang (2002, 2009) and Krammer and Lange-Bertalot (1986). Ecological interpretation and pH preferences for each species were adopted from Charles (1985), Van Dam et al. (1994), Wu et al. (1997), and Chen and Wu (1999). Bio-stratigraphic diagrams and cluster analysis were conducted using C2 software (Juggins 2007), TILIA, and TILIA-GRAPH programs (Grimm 1993).

Ordination analysis, a numerical technique applied to community data for detecting changes in the dynamics, structure and function of ecosystems, was used to extract important variables, such as temperature, water quality, and nutrients, that correlated with the distribution of diatom species. The ordination analysis was performed using CANOCO version 4.5 (ter Braak and Smilauer 2002).

Subsequently, the main factors controlling the diatom composition in TFL were determined by a linear ordination method, principal component analysis (PCA), to acquire environmental information from diatom assemblages. Only those species with an average abundance >5 % were included in the analysis. Diatom data were scaled on inter-species correlation and the species scores were divided by the standard deviation. Species data were not transformed or centered by species without standardization.

In this study, diatom-based transfer functions (DITF) from the European Diatom Database Initiative (EDDI) were used to infer pH. Validation of this approach was done before proceeding. Results showed that ~75–90 % of taxa in TFL sediment samples matched those in the EDDI training set (web verification program, http://craticula.ncl.ac.uk/Eddi/jsp/verify.jsp). This satisfied the criterion of >75 % suggested by Birks (1998) and indicated that the DITF of the EDDI was applicable to TFL, similar to its application in eastern China (Li et al. 2010).

Next, estimates of diatom-inferred pH were made using transfer functions derived from the web-based European Diatom Database system (EDDI) (Juggins 2001; Gil-Romera et al. 2009). To achieve this, EDDI transfer functions for pH reconstruction were developed using weighted averaging (WA), weighted averaging partial least squares (WAPLS; only for DI-pH), modern analog techniques (MAT), and locally-weighted weighted averaging (LWWA). Before using these methods, a test of their suitability for TFL was done. All exhibited similar trends in the TFL samples. The data inferred using LWWA, however, displayed the lowest root mean square error RMSE (0.38), indicating it was more reliable than the others (Juggins 2001; Li et al. 2010). Moreover, the LWWA-based DI-pH for surface sediment samples (average = 5.89) was close to the measured value for modern lake waters (mean = 5.86, 2008–2010). Thus, the LWWA method was used for pH inference in TFL.

We made inter-site comparisons of the DI-pH data between TFL and Duck Pond (25°10′N, 121°33′E, 760 m a.s.l.), northern Taiwan (Chen et al. 2009), Yuanyang Lake (24°35′N, 121°24′E, 1,670 m a.s.l.), northeastern Taiwan (Chen and Wu 1999), and Great Ghost Lake (22°52′N, 120°51′E, 2,200 m a.s.l.), southern Taiwan (Wu et al. 1997).

Samples for geochemical analysis were weighed and freeze-dried. Dried samples were ground and acidified to remove carbonate. Samples were then packed in tin capsules and combusted in an elemental analyzer connected to a Thermo DELTA V isotope ratio mass spectrometer. Measures of TOC, TN, $\delta^{13}C$ and $\delta^{15}N$ were obtained simultaneously on each sample. Carbon isotope ratios are presented using standard δ notation with respect to PDB, and $\delta^{15}N$ are expressed relative to the air standard. MS was determined using a Bartington MS2C at intervals of 0.5 cm.

Results

Chronology

Dating results are given in Table 1 and Fig. 3. There are 12 ^{210}Pb dates for the upper 6 cm of the core and four ^{14}C dates deeper in the core. Radiocarbon dates are in order and there appears to have been continuous sediment accumulation. The 55.5-cm-long sediment core covers the period from AD 490 to present. The calculated sedimentation rate ranged between 0.19 and 0.65 mm/year, with the highest values measured near the sediment surface and lowest values in the deeper, early part of the record.

Diatom analysis

A total of 54 diatom species was recorded in the studied TFL sediment core. They are the same taxa found in the surface sediment (data not shown), indicating that there was little change in taxa present over last 1,500 years. The verification program of the EDDI website showed that >75 % of the taxa that occurred in the TFL core are found in the EDDI dataset.

Using the pH preference of taxa, three main groups were identified, namely alkaliphilous (*Achnanthidium minutissimum*, *Encyonopsis microcephala*, *Staurosira elliptica*), circum-neutral (*Eunotia praerupta*, *Gomphonema gracile*, *Navicula lanceolata*), and acidophilous (*Aulacoseira distans*, *Eunotia bilunaris* var. *mucophila*, *E. paludosa*, *Frustulia rhomboides* var. *crassinervia*, *Neidium alpinum*, *N. ampliatum*, *Pinnularia gibba*, *P. microstauron*, *Surirella linearis*). Applying cluster analysis to the diatom assemblages, two main diatom zones were differentiated. Diatom zone I consisted of two sub-zones, whereas zone II consisted of three sub-zones (Fig. 4).

In diatom zone Ia (55.5–43.5 cm, AD 490–1110), the acidophilous species *A. distans* was dominant (42–76 %). The circum-neutral species *N. lanceolata* was common during the early period, but was replaced by another circum-neutral species in the latter period. Few alkaliphilous species were present throughout this zone.

In diatom zone Ib (43.5–28 cm, AD 1110–1470), the acidophilous species, *A. distans*, was present in high relative abundance (45–79 %), whereas the abundance of both the circum-neutral and alkaliphilous species increased slightly at 35 cm (ca. AD 1350).

In diatom zone IIa (28–19 cm, AD 1470–1640), *A. distans* was replaced by the alkaliphilous species *E. microcephala*, in association with an increase in circum-neutral species. In diatom zone IIb (19–6 cm, AD 1640–1910), the remarkable succession between *A. distans* and *E. microcephala* occurred again. In diatom zone IIc (6–0 cm, AD 1910 to present), *A. distans* was again dominant. Additionally, the

Table 1 ^{14}C AMS ages and the calibrated ages of the sediments from TFL

Depth (cm)	Lab no.	Materials	δ^{13}C (‰)	^{14}C age (BP)	Calibrated age[a] (cal BP)
22.5–23	NZA 32825	Plant fragment	−28.0	323 ± 20	308–460
34.5–35.0	NZA 33630	Plant fragment	−26.8	495 ± 35	555–611
43.5–44.0	NZA 33600	Plant fragment	−27.5	973 ± 25	795–875
53.5–54.0	NZA 32827	Plant fragment	−25.5	1,502 ± 20	1,335–1,413

[a] Derived from Reimer et al. (2004). 0 cal BP = 1950 AD

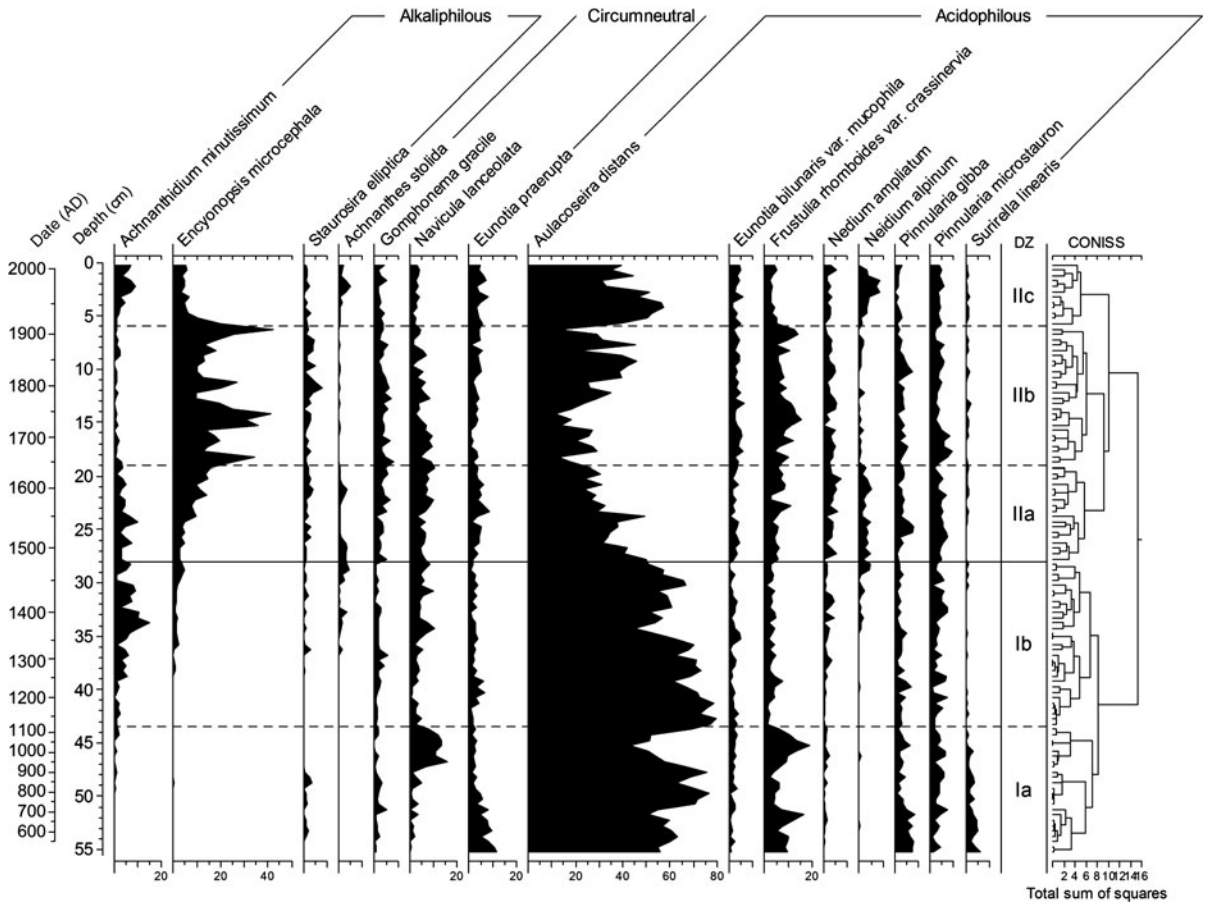

Fig. 4 Sediment profiles of dominant acidophilous, circumneutral, and alkaliphilous diatoms in TFL

circum-neutral and alkaliphilous species increased slightly in the uppermost 2 cm.

Geochemical analysis

Results of the geochemical analysis and MS are presented in Fig. 5. TOC fluctuated between 1.0 and 4.0 % (mean = 3.0 %), while TN varied between 0.1 and 0.4 % (mean = 0.3 %) throughout the core. Both values declined significantly in diatom zone IIc and were higher near the sediment surface, displaying similar stratigraphic fluctuations. The C/N ratio ranged between 6.8 and 13.3 (mean = 11.0), being higher in the upper part of zone IIa and lower in zone IIc.

In zone Ia, the δ^{13}C values were as low as −27 ‰, whereas they increased near the end of IIa and were low toward the beginning of zone Ib. Throughout zone Ib, δ^{13}C values fluctuated slightly, between −26.2 and 27.0 ‰. In zone IIa, the values fluctuated more and

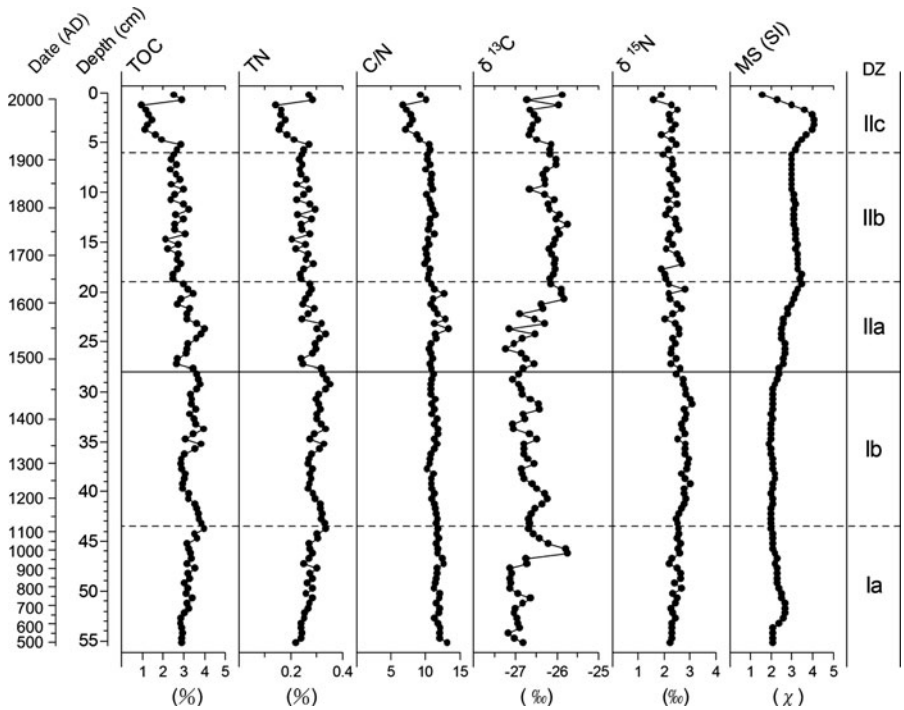

Fig. 5 Fluctuations in TOC, TN, C/N ratio, $\delta^{13}C$, $\delta^{15}N$ and magnetic susceptibility (MS) with respect to the diatom zones in the TF-2 sediment core

exhibited an increase toward IIb, in which they were higher than in other zones and changed only slightly, between 26.5 and −25.7 ‰. In zone IIc, the values declined and fluctuated near the sediment surface. The $\delta^{15}N$ values in the sediments ranged between 1.6 and 3.1 ‰ (mean = 2.5 ‰), being higher in diatom zones Ia and Ib and lower in zones IIa, IIb and IIc.

MS values ranged from 4.1 to 1.6 (mean = 2.6) throughout the core. The values in diatom zone I were lower than in zone IIa. The MS values showed little change in diatom zone IIb, were elevated in zone IIc, and decreased in the upper part toward the sediment surface (Fig. 5).

Principal component analysis and diatom-inferred pH

Ordination analysis was used to extract important variables that correlated with the distribution of diatom species. Before the analysis, an indirect ordination approach, i.e. detrended correspondence analysis (DCA), was used to determine whether a linear or a unimodal model was most suitable for our study. Results indicated that the gradient length was 1.6 (< 2.0 standard deviations), suggesting that a linear model was appropriate for the diatom assemblages in TFL.

PCA was conducted to identify the factors controlling diatom community composition. The summary of PCA results and the environmental meaning of the selected diatom species (Table 2) indicated that PC1 explained 84 % of the variability, while the acidophilous diatom *A. distans* had the lowest values, suggesting negative correlation between PC1 and pH. Figure 6 shows the plots of sediment samples for the PC1 axis and PC2 axis in the PCA analysis. Samples from zones Ia and Ib had negative values for PC1. By contrast, most of the samples from zones IIa, IIb, and IIc had positive values for PC1.

Values of DI-pH throughout the core are shown in Fig. 7. The DI-pH ranged from 5.4 to 6.8 (mean = 5.8) and exhibited a change pattern similar to PC1. Over zone Ia and Ib, the DI-pH fluctuated slightly around 5.5, after which it increased remarkably from IIa to IIb. Close to the sediment surface, namely in IIc, the DI-pH values decreased to about 5.8 and changed little.

Discussion

Aulacoseira distans was the predominant taxon throughout the core. This species is planktonic in shallow waters <4 m deep, but can be classified as a

Table 2 Scores of PCA and indication of environmental conditions for the selected diatom species in the sediments of TFL

	PC1	PC2	Environmental indication	
			pH	Trophic state preference
Variable (%)	84	7		
E. praerupta	0.04	−0.09	Circumneutral	Oligotrophic
G. gracile	0.64	0.01	Circumneutral	Eutrophic
N. lanceolata	0.32	−0.42	Circumneutral	Broad
A. distans	−0.99	0.11	Acidophilous	Oligotrophic
E. bilunaris var. *mucophila*	0.46	−0.11	Acidophilous	Eutrophic
E. paludosa	0.62	−0.21	Acidophilous	–
F. rhomboides var. *crassinervia*	0.51	0.16	Acidophilous	Oligotrophic
N. ampliatum	0.56	−0.35	Acidophilous	–
N. alpinum	0.23	−0.52	Acidophilous	–
P. gibba	−0.01	−0.14	Acidophilous	Broad
P. microstauron	0.23	−0.27	Acidophilous	Oligotrophic
S. linearis	−0.20	0.05	Acidophilous	Broad
A. minutissimum	−0.04	−0.51	Alkaliphilous	Broad
E. microcephala	0.87	0.48	Alkaliphilous	Oligotrophic
S. elliptica	0.53	0.11	Alkaliphilous	Eutrophic

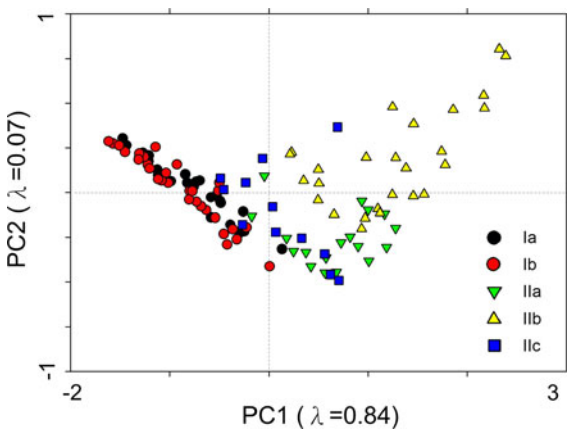

Fig. 6 Plot of the first axis (PC1) versus the second axis (PC2) of the PCA of sediment samples from TFL

benthic species (Brugam et al. 1998; Moos et al. 2005). In diatom zone II, the dominance of this species declined to some degree, associated with an increase in the subdominant species, *E. microcephala*, which occupies epilithic or epiphytic habitats. Dominance of one or the other species implies there was a change in water depth from zone I to zone II. Our observations of the contemporary lake water showed that the water level of TFL changes rapidly. It is high (5–8 m deep) during the monsoon season and low (<4 m) during the dry season. Thus, the change in habitat availability was probably related to the amount of precipitation.

TFL is an inland lake with no surface outlet and possesses a yellow cypress forest in its watershed. The pH of the lake surface water is directly related to precipitation. Our field measurements show the pH of lake water is higher during the rainy season. The pH of the lake surface water is lower in the dry season (pH 4.5–5.5) and slightly alkaline (pH 7.0–7.3) in the wet season. The pH of precipitation (5.0–6.5) is intermediate. Thus, other factors must influence lake pH.

TFL is an oligotrophic to mesotrophic lake, with relatively high chlorophyll *a* content in the wet season. Greater photosynthetic activity of algae in the wet season, i.e. withdrawal of CO_2, raises the pH of the water. Thus, higher pH in the wet season reflects the combined effects of amount of precipitation and groundwater and photosynthetic activity of phytoplankton. Higher productivity, inferred from chlorophyll *a* content, was measured in wet seasons during our recent study of TFL. Thus, amount of precipitation serves as an index of pH in this lake.

Prior to AD 500 (diatom zone I), there was no contribution to acid rain from anthropogenic sources or any remarkable natural events that would have affected the pH of precipitation. Thus, low DI-pH at that time was likely a result of low precipitation. Over the time

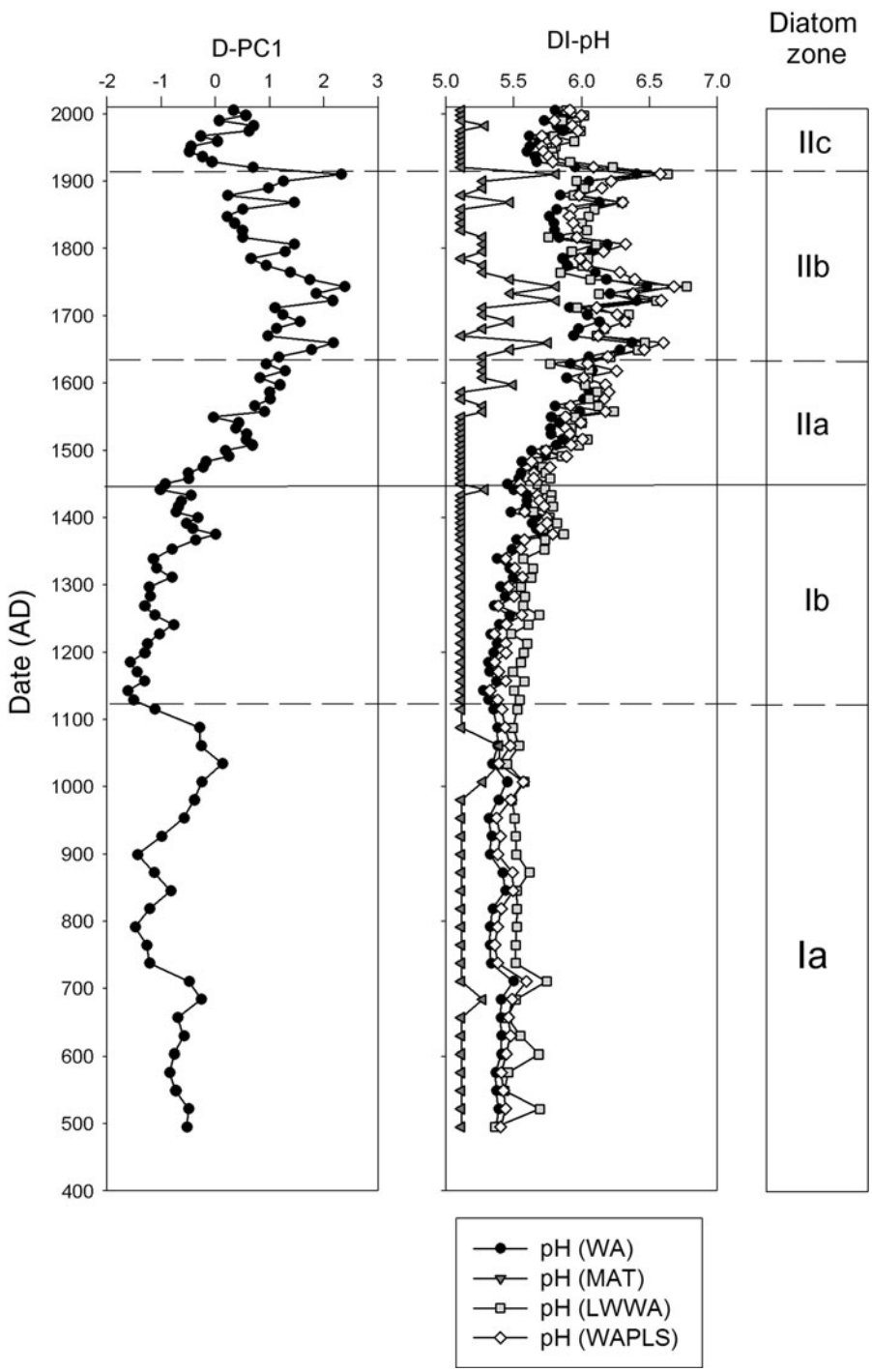

Fig. 7 Fluctuations in principal component 1 (PC1) and diatom-inferred pH (DI-pH) with respect to different diatom zones. Methods for inferring the pH are given below each *panel* in the figure

span from diatom zone Ib to IIb, there was a gradual increase in DI-pH, which indicates greater precipitation. Throughout the entire core, there were four decadal periods with apparently higher precipitation, beginning ca. AD 1660, 1730, 1820 and 1920 (Fig. 7).

Synchronous increases in DI-pH, MS and $\delta^{13}C$, along with a decline in $\delta^{15}N$ in diatom zone II, probably indicate intense erosion and increased soil input from the watershed, suggesting events of high rainfall. Soils are thought to be the primary source of

organic matter in the sediment (Kao and Liu 2000). A *t* test on $\delta^{13}C$ and $\delta^{15}N$ values revealed a significant difference between zones Ib and IIb ($p < 0.001$), indicating differences in organic matter input between these two time periods. All lines of evidence point to a change in precipitation amount over the studied period of time (Fig. 8).

Since AD 1920, there has been a decline in DI-pH, suggesting acidification of this lake. A number of alpine lakes have become acidified since AD 1900 (Chen et al. 2004). Furthermore, historic documents indicate that there has been deforestation of the mountains near TFL since AD 1906 (Lin 1996). This activity caused the declines in TOC and N content and the increase in MS values in the lake sediments (Fig. 5). Thus, the declining pH of TFL in the last century may have been a consequence of both increased input of acid deposition and forest removal in the basin.

The East Asia Monsoon has been weak since AD 350, as reflected in the drier climate in the middle and high latitudes in China (An et al. 2000; Cosford et al. 2008; Hu et al. 2008). Precipitation in the East Asia monsoon region, however, varied spatially and temporally during the LIA. A synthesis of 1,500 years of historical records in China indicated there were 16 droughts and 18 floods during the LIA, far more than during other periods. Furthermore, the droughts and floods occurred non-synchronously across latitudes, reflecting local differences (Zheng et al. 2006). Comparison of DI-pH data from four Taiwanese alpine lakes shows that there was inter-site variation in inferred acidity over the LIA (Fig. 9). In Duck Pond, northern Taiwan, DI-pH was high in the early LIA and declined after AD 1680. These changes were related to relatively higher and lower precipitation, respectively (Chen et al. 2009). In Yuanyang Lake, the input of acid runoff from the watershed was related to the magnitude of precipitation (Yang et al. 2011). Thus, increased acidity inferred after AD 1410 and 1680 could have been a consequence of increased precipitation in the late LIA (Chen and Wu 1999). In southern Taiwan, the geochemical records of Great Ghost Lake indicated that the climate was cool and dry (Lou et al. 1997), though values of DI-pH fluctuated to some degree in the LIA period. Despite regional variability in DI-pH through the LIA, DI-pH in these four Taiwanese lakes shows a synchronous decline since ca. AD 1900, suggesting widespread lake acidification in Taiwan during the last century.

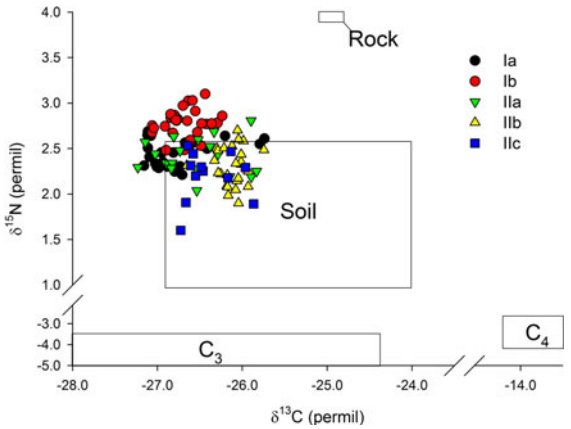

Fig. 8 The $\delta^{13}C$-$\delta^{15}N$ plot of the sediment samples. The $\delta^{13}C$-$\delta^{15}N$ ranges of C3, C4, rock and soil were determined according to the method described by Kao and Liu (2000)

Yao et al. (2000) suggested that the seventeenth century was the coldest period of the LIA in western China, according to $\delta^{18}O$ values from the Dunde ice core in the Qilian Mountains. Wet climate was inferred for the period AD 1330–1850 in the Yangtze River region of eastern China, from a decline in the palynological aridity index (Yi et al. 2006). According to historical weather records from northern Japan, the cold phases of the LIA occurred during AD 1611–1650, 1691–1720 and 1821–1850 (Maejima and Tagami 1983). These cold periods correspond well with the increased precipitation events inferred from TFL in the present study. In the European region, the climax of the LIA occurred in AD 1650–1750, related to an abnormal solar event, the so-called Maunder Minimum (Bond et al. 2001).

Solar variability is one of the driving forces of climate change and affects both the Asian and Indian monsoons at decadal to multi-decadal timescales (Neff et al. 2001; Mehta and Lau 1997; Wang et al. 2005). In Taiwan, total annual precipitation is highly correlated with monsoon rainfall. In the northeastern part of Taiwan, most precipitation is contributed by summer typhoons (July and August) and late-season typhoons (September and October) (Chen and Chen 2003). In the present study, elevated precipitation during the late LIA is thought to have been caused by increased typhoon events. The comparison of four Taiwanese subalpine lakes shows that changes in DI-pH exhibit similar patterns to shifts in solar irradiance during the

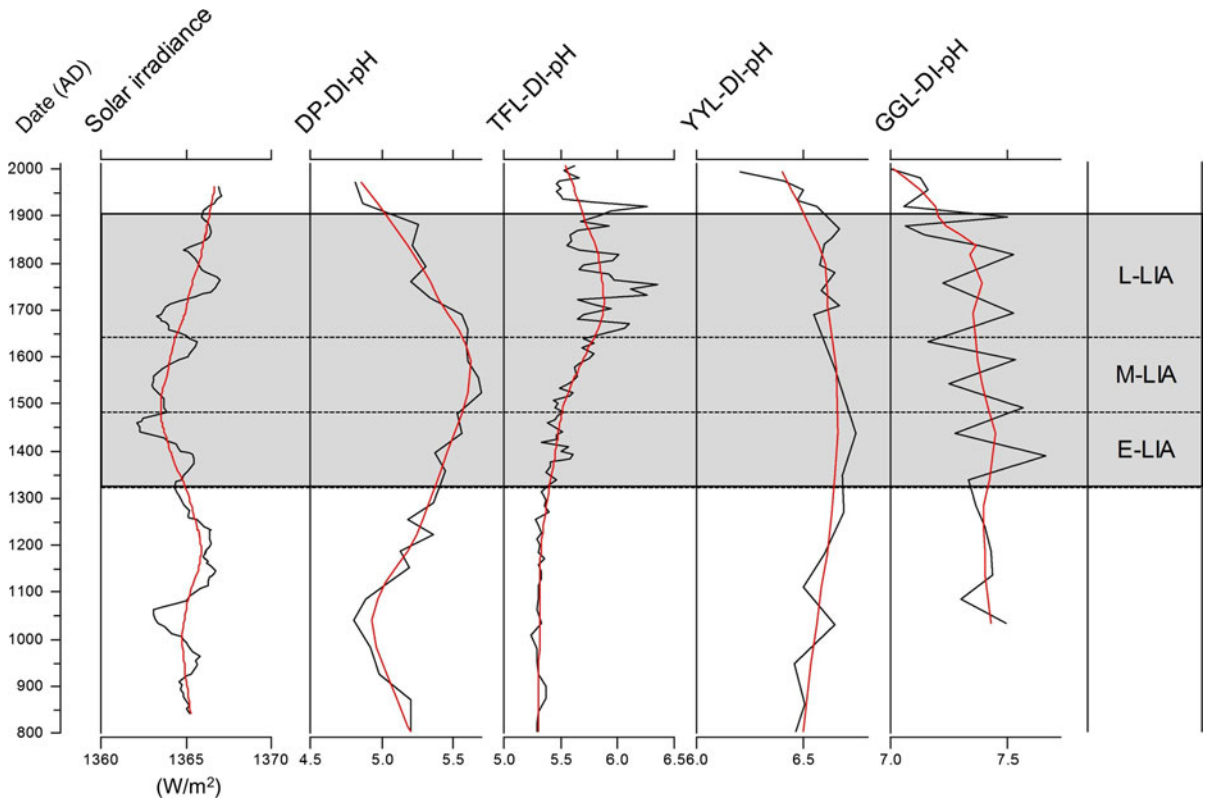

Fig. 9 Comparison of solar irradiance (Bard et al. 2000) and rainfall-correlated DI-pH in Duck Pond (*DP*), Tsuifong Lake (*TFL*), Yuanyang Lake (*YYL*) and Great Ghost Lake (*GGL*) during the past 1,200 years

late LIA (Bard et al. 2000). The increased solar irradiance is associated with changes in the summer monsoon intensity, i.e. more or stronger typhoon events in the past (Wan et al. 2011). The study of runoff from the watershed in Yuanyang Lake shows that erosion is strongly correlated with precipitation (Yang et al. 2011). Thus, we infer that increased acidity of lake water is related to high soil erosion as a result of elevated monsoon precipitation, which in turn is related to the intensity of solar irradiance.

Conclusions

This paleolimnological study presented evidence for elevated precipitation during the late LIA in northeastern Taiwan. The increased acidity of lake water, erosion and consequent soil input at TFL between AD 1640 and AD 1920 are attributed to an increase in precipitation that was correlated with intense solar irradiance. Anthropogenic lake acidification, a consequence of acid rain, occurred synchronously across Taiwanese alpine lakes beginning in the early 1900s. In addition, deforestation caused elevated runoff from the TFL watershed and contributed to acidification. Our results provide evidence of shifts in monsoon climate across northeastern Taiwan during the LIA.

Acknowledgments We thank Dr. Shuh-Ji Kao of the Research Center for Environmental Changes, Academia Sinica for suggestions regarding geochemical analysis and providing water quality data. The authors appreciate the financial support provided by a grant from the National Science Council (NSC97-2621-B-002-MY3, NSC101-2116-M-002-007-, NSC101-2811-M-002-140-), Interchange Association, Japan, and German Academic Exchange (99-2911-I-002-059-2). Dr. K. Kashima, Laboratory of Kyushu University, Japan is acknowledged for allowing a portion of the study to be conducted in that laboratory.

References

An Z, Porter SC, Kutzbach JE, Wu X, Wang S, Liu X, Li X, Zhou W (2000) Asynchronous Holocene optimum of the East Asian monsoon. Quat Sci Rev 19:743–762

Atwater B, Furukawa R, Hemphill-Haley E, Ikeda Y, Kashima K, Kawase K, Kelsey H, Moore A, Nanayama F, Nishimura Y (2004) Seventeenth-century uplift in eastern Hokkaido, Japan. Holocene 14:487

Bard E, Raisbeck G, Yiou F, Jouzel J (2000) Solar irradiance during the last 1200 years based on cosmogenic nuclides. Tellus B 52:985–992

Binford M (1990) Calculation and uncertainty analysis of ^{210}Pb dates for PIRLA project lake sediment cores. J Paleolimnol 3:253–267

Birks HJB (1998) D.G. Frey and E.S. Deevey Review #1: numerical tools in palaeolimnology—progress, potentialities, and problems. J Paleolimnol 20:307–332

Bond G, Kromer B, Beer J, Muscheler R, Evans MN, Showers W, Hoffmann S, Lotti-Bond R, Hajdas I, Bonani G (2001) Persistent solar influence on North Atlantic climate during the Holocene. Science 294:2130–2136

Borromei AM, Coronato A, Franzén LG, Ponce JF, Sáez JAL, Maidana N, Rabassa J, Candel MS (2010) Multiproxy record of Holocene paleoenvironmental change, Tierra del Fuego, Argentina. Palaeogeogr Palaeoclimat Palaeoecol 286:1–16

Bradley RS, Jonest PD (1993) "Little Ice Age" summer temperature variations: their nature and relevance to recent global warming trends. Holocene 3:367–376

Brugam RB, McKeever K, Kolesa L (1998) A diatom-inferred water depth reconstruction for an Upper Peninsula, Michigan, lake. J Paleolimnol 20:267–276

Charles DF (1985) Relationships between surface sediment diatom assemblages and lakewater characteristics in Adirondack Lakes. Ecology 66:994–1011

Chen CS, Chen YL (2003) The rainfall characteristics of Taiwan. Month Weather Rev 131:1323–1341

Chen SH, Wu JT (1999) Paleolimnological environment indicated by the diatom and pollen assemblages in an alpine lake in Taiwan. J Paleolimnol 22:149–158

Chen CTA, Wu JT, Wang BJ, Huang KM (2004) Acidification and trace metals of lakes in Taiwan. Aquat Geochem 10: 33–57

Chen J, Wan G, Zhang DD, Chen Z, Xu J, Xiao T, Huang R (2005) The "Little Ice Age" recorded by sediment chemistry in Lake Erhai, southwest China. Holocene 15:925–931

Chen SH, Wu JT, Yang TN, Chuang PP, Huang SY, Wang YS (2009) Late Holocene paleoenvironmental changes in subtropical Taiwan inferred from pollen and diatoms in lake sediments. J Paleolimnol 41:315–327

Chu G, Liu J, Sun Q, Lu H, Gu Z, Wang W, Liu T (2002) The "Mediaeval Warm Period" drought recorded in Lake Huguangyan, tropical South China. Holocene 12:511–516

Cosford J, Qing H, Eglington B, Mattey D, Yuan D, Zhang M, Cheng H (2008) East Asian monsoon variability since the Mid-Holocene recorded in a high-resolution, absolute-dated aragonite speleothem from eastern China. Earth Planet Sci Lett 275:296–307

Gil-Romera G, Grimm E, Huntley B, Kunes P, Kühl N, Leydet M, Lotter A, Tarasov P, Tonkov S, Fyfe R (2009) The European Pollen Database: past efforts and current activities. Veget Hist Archaeobot 18:417–424

Grimm E (1993) TILIA: a pollen program for analysis and display. Illinois State Museum, Springfield

Grove JM (1988) The Little Ice Age. Methuen and Company, London

Hu C, Henderson GM, Huang J, Xie S, Sun Y, Johnson KR (2008) Quantification of Holocene Asian monsoon rainfall from spatially separated cave records. Earth Planet Sci Lett 266:221–232

Juggins S (2001) The European Diatom Database user guide, version 1.0. University of Newcastle, UK

Juggins S (2007) C2 Version 1.5: software for ecological and palaeoecological data analysis and visualization. Newcastle University, Newcastle upon Tyne

Kao SJ, Liu KK (2000) Stable carbon and nitrogen isotope systematics in a human-disturbed watershed (Lanyang-Hsi) in Taiwan and the estimation of biogenic particulate organic carbon and nitrogen fluxes. Global Biogeochem Cycles 14:189–198

Kashima K (2003) The quantitative reconstruction of salinity changes using diatom assemblages in inland saline lakes in the central part of Turkey during the Late Quaternary. Quat Int 105:13–19

Krammer K, Lange-Bertalot H (1986–1991) Süßwasserflora von Mitteleuropa: Bacillariophyceae. Gustav Fisher Verlag Stuttgart, pp 1–4

Li YM, Ferguson D, Wang YF, Li CS (2010) Paleoenvironmental inferences from diatom assemblages of the middle Miocene Shanwang Formation, Shandong, China. J Paleolimnol 43:799–814

Lin QC (1996) The development history of Taiping Mountain. Fulunxiaozhu, Ilan County (in Chinese)

Lin JM, Wang WL, Wang LC, Lee MY, Lee TQ, Wei KY (2003) Quaternary oceanographic changes, based on the diatom fossil record in the piston core MD972144 in the South China Sea. West Pac Earth Sci 3:119–132

Lin SF, Liew PM, Lai TH (2004) Late Holocene pollen sequence of the Ilan Plain, northeastern Taiwan and its environment and climatic implications. Terr Atmos Ocean Sci 15:111–132

Lin SF, Huang TC, Liew PM, Chen SW (2007) A palynological study of environmental changes and their implication for prehistoric settlement in the Ilan Plain, northeastern Taiwan. Veg Hist Archaeobot 16:127–138

Lou JY, Chen CTA, Wann JK (1997) Paleoclimatological records of the Great Ghost Lake in Taiwan. Sci China Ser D Earth Sci 40:284–292

Maejima I, Tagami Y (1983) Climate of little ice age in Japan. Geogr Rep Tokyo Metrop Univ 18:91–111

Mao JJ (2006) Investigation on the biological resources and habitat of Tsuei-Feng Lake. Res Conserv For Bureau 94-10, 51 pp (in Chinese)

Mehta VM, Lau KM (1997) Influence of solar irradiance on the Indian monsoon-ENSO relationship at decadal-multidecadal time scales. Geophys Res Lett 24:159–162

Moos M, Laird K, Cumming B (2005) Diatom assemblages and water depth in Lake 239 (Experimental Lakes Area,

Ontario): implications for paleoclimatic studies. J Paleolimnol 34:217–227
Neff U, Burns SJ, Mangini A, Mudelsee M, Fleitmann D, Matter A (2001) Strong coherence between solar variability and the monsoon in Oman between 9 and 6 kyr ago. Nature 411:290–293
Nelson A, Jennings A, Kashima K (1996) An earthquake history derived from stratigraphic and microfossil evidence of relative sea-level change at Coos Bay, southern coastal Oregon. Geol Soc Am Bull 108:141–154
Nesje A, Dahl SO (2003) The "Little Ice Age"—only temperature? Holocene 13:139–145
Rasmussen LA, Andreassen LM, Baumann S, Conway H (2010) "Little Ice Age" precipitation in Jotunheimen, southern Norway. Holocene 20:1039–1045
Reimer PJ, Baillie MGL, Bard E, Bayliss A, Beck JW, Bertrand CJH, Blackwell PG, Buck CE, Burr GS, Cutler KB (2004) IntCal04 terrestrial radiocarbon age calibration, 0–26 Cal Kyr BP. Radiocarbon 46:1029–1058
Saegusa Y, Sugai T, Ogami T, Kashima K, Sasao E (2011) Reconstruction of Holocene environmental changes in the Kiso-Ibi-Nagara compound river delta, Nobi Plain, central Japan, by diatom analyses of drilling cores. Quat Int 230:67–77
Schütt B, Berking J, Frechen M, Frenzel P, Schwalb A, Wrozyna C (2010) Late Quaternary transition from lacustrine to a fluvio-lacustrine environment in the north-western Nam Co, Tibetan Plateau, China. Quat Int 218:104–117
Shinneman A, Edlund M, Almendinger J, Soninkhishig N (2009) Diatoms as indicators of water quality in Western Mongolian lakes: a 54-site calibration set. J Paleolimnol 42:373–389
Shinneman A, Bennett D, Fritz S, Schmieder J, Engstrom D, Efting A, Holz J (2010) Inferring lake depth using diatom assemblages in the shallow, seasonally variable lakes of the Nebraska Sand Hills (USA): calibration, validation, and application of a 69-lake training set. J Paleolimnol 44:443–464
Smol JP, Birks HJB, Last WM (2001) Tracking environmental change using Lake sediments. Vol. 3: terrestrial, algal, and siliceous indicators. Kluwer, Dordrecht, p 371
Stoermer EF, Smol JP (1999) The diatoms. Applications for the environmental and earth sciences. Cambridge University Press, Cambridge, p 469
Stuiver M, Reimer PJ, Reimer RW (2005) CALIB 5.0. WWW program and documentation, Quaternary Research Center, University of Washington, Seatle
ter Braak CJF, Smilauer P (2002) Canoco 4.5: reference manual and Canodraw for Windows. User's Guide: software form canonical community ordination (version 4.5). Microcomputer Power, Ithaca, p 500
Van Dam H, Mertens A, Sinkeldam J (1994) A coded checklist and ecological indicator values of freshwater diatoms from The Netherlands. Aquat Ecol 28:117–133
Villalba R (1994) Tree-ring and glacial evidence for the medieval warm epoch and the little ice age in southern South America. Clim Change 26:183–197
Wan NJ, Li HC, Liu ZQ, Yang HY, Yuan DX, Chen YH (2011) Spatial variations of monsoonal rain in eastern China: instrumental, historic and speleothem records. J Asia Earth Sci 40:1139–1150
Wang Y, Cheng H, Edwards RL, He Y, Kong X, An Z, Wu J, Kelly MJ, Dykoski CA, Li X (2005) The Holocene Asian monsoon: links to solar changes and north Atlantic climate. Science 308:854–857
Wang LC, Lee TQ, Chen SH, Wu JT (2010) Diatoms in Liyu Lake, eastern Taiwan. Taiwania 55:228–242
Wang LC, Wu JT, Lee TQ, Lee PF, Chen SH (2011) Climate changes inferred from integrated multi-site pollen data in northern Taiwan. J Asia Earth Sci 40:1164–1170
Wiklund J, Bozinovski N, Hall R, Wolfe B (2010) Epiphytic diatoms as flood indicators. J Paleolimnol 44:25–42
Wu JT, Wang YF (2002) Diatoms of the Mystery Lake, Taiwan (I). Taiwania 47:71–96
Wu JT, Wang YF (2009) Diatoms of the Mystery Lake, Taiwan (III). Taiwania 54:231–240
Wu JT, Chuang PP, Wu LZ, Chen CTA (1997) Diatoms as indicators of environmental changes: a case study in Great Ghost Lake. Proc Nat Sci Counc Repub China Part B Life Sci 21:112–119
Wu JT, Chang SC, Wang YS, Wang YF, Hsu MK (2001) Characteristics of the acidic environment of the Yuanyang Lake. Bot Bull Acad Sin 42:17–22
Yang TN, Lee TQ, Meyers PA, Fan CW, Chen RF, Wei KY, Chen YG, Wu JT (2011) The effect of typhoon induced rainfall on settling fluxes of particles and organic carbon in Yuanyang Lake, subtropical Taiwan. J Asia Earth Sci 40:1171–1179
Yao T, Wang N, Shi Y (2000) Climate and environment changes derived from ice core records. In: Shi Y (ed) Glaciers and their environments in China—the present, past and future. Science Press, Beijing, pp 285–319 (in Chinese)
Yi S, Saito Y, Chen Z, Yang D (2006) Palynological study on vegetation and climatic change in the subaqueous Changjiang (Yangtze River) delta, China, during the past about 1600 years. Geosci J 10:17–22
Zheng J, Wang W, Ge Q, Man Z, Zhang P (2006) Precipitation variability and extreme events in eastern China during the past 1500 years. Terr Atmos Ocean Sci 17:579